Supplemental Material: Phase-controlled bistability of a dark soliton train in a polariton fluid

V. Goblot,[1] H. S. Nguyen,[2] I. Carusotto,[3] E. Galopin,[1] A. Lemaître,[1] I. Sagnes,[1] A. Amo,[1] and J. Bloch[1,4]

[1] *Centre de Nanosciences et de Nanotechnologies, CNRS, Univ. Paris-Sud, Université Paris-Saclay, C2N - Marcoussis, 91460 Marcoussis, France*
[2] *Institut de Nanotechnologies de Lyon, Ecole Centrale de Lyon, CNRS (UMR 5270), 69134 Ecully, France*
[3] *INO-CNR BEC Center and Dipartimento di Fisica, Università di Trento, I-38123 Povo, Italy*
[4] *Département de Physique, Ecole Polytechnique, Université Paris Saclay, F-91128 Palaiseau Cedex, France*

(Dated: October 18, 2016)

I - PHASE OF THE POLARITON FLUID

In contrast to ultracold atomic gases, it is possible to directly access the phase of the polariton fluid *in situ* by interferometric techniques. We use the pump laser beam, which has a constant phase, as a reference and we overlap this constant-phase reference beam with the real space emission from the wire (see Fig. S1(a)). The phase of the polariton fluid can then be extracted from the resulting interferogram. In particular, a phase jump of π can be detected in the interference pattern as a discontinuity in the fringes. Fig. S1(c) presents an interference pattern measured with a high pumping power for the polariton fluid, i.e., in the nonlinear regime. With the choice of experimental parameters here, a single soliton is present in the wire, as shown in Fig. S1(b). A π phase jump across the soliton is clearly evidenced in the interferogram, at the position indicated by the white arrows.

We emphasize, however, that measuring this phase jump of π is not sufficient to ascertain that the density dip in the nonlinear regime is indeed a dark soliton. As mentioned in the main text, in the linear regime, a standing wave is formed between the pumping spots. Hence, also in the linear regime, there is a π phase jump across each density dip, i.e., between each two nodes of the standing wave, as shown in Fig. S1(d),(e), for example at the position indicated by the white arrows. The nonlinear nature of the dark solitons present at high pumping power is confirmed mainly by their abrupt generation and expulsion in both power and phase scans, as shown in the main text. The presence of the π phase jump is a mere sanity check.

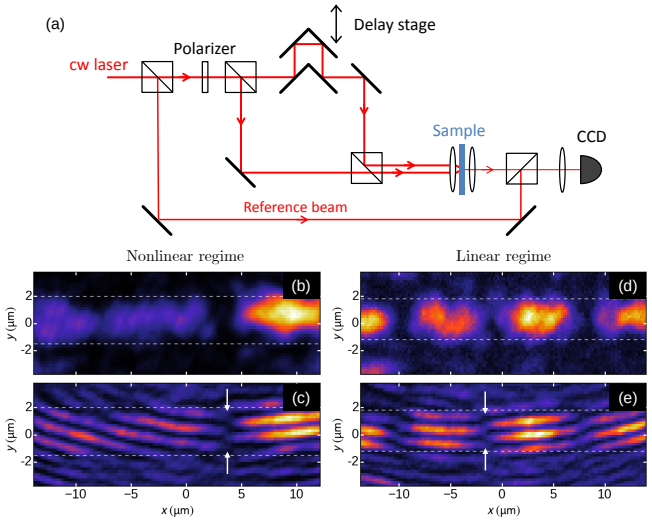

FIG. S1. (a) Sketch of the experimental setup used to measure the phase of the polariton fluid. (b) Real space emission profile and (c) corresponding interferogram of the wire, in the nonlinear regime. A phase jump of π is clearly visible at the position of the soliton, indicated by the white arrows. (d) Real space emission profile and (e) corresponding interferogram in the linear regime. A phase jump of π is also observed around each node of the standing wave pattern, see, e.g., the position indicated by the white arrows.

II - SOLITON PROFILE

As discussed in the main text, the solution of the Gross-Pitaevskii equation determining the profile of a

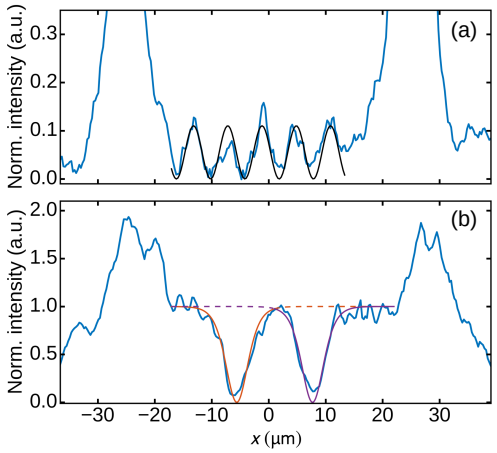

FIG. S2. (a) Density profile in the linear regime, corresponding to Fig. 1(d) of the main text, fitted by a cosine function (black line). (b) Density profile in the nonlinear regime, corresponding to Fig. 2(b) of the main text. The orange (resp. purple) line is a fit of the left (right) soliton. Dashed lines indicate regions where the fits are not valid due to the presence of the second soliton.

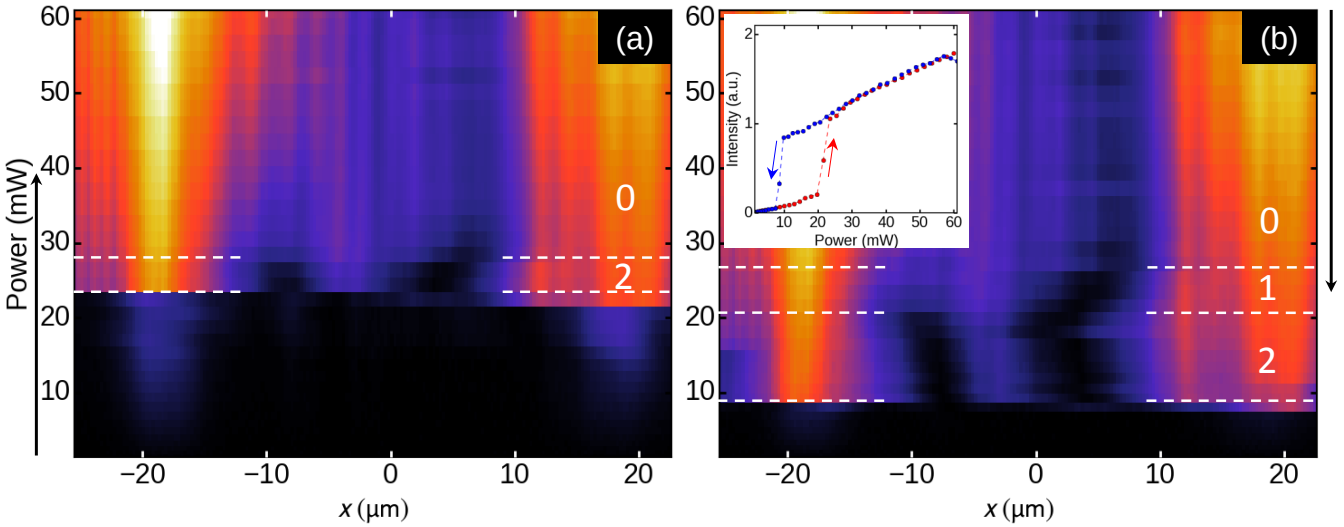

FIG. S3. (a) Integrated density profile measured as a function of pump power, for an increasing pump power. The number of solitons in the wire for a power range over which it remains constant is indicated in white. $\Delta E = 0.27$ meV, $d = 40$ μm and $\Delta\varphi \approx 0$ (but non zero). (b) Power scan with the same parameters, but for a decreasing pump power. Inset: Total intensity in the wire for the upward (red dots) and downward (blue dots) pump power scans.

soliton train is an elliptic function [1]. In the case of a profile with a single dark soliton, the density evolves as $n(x) = \tanh^2((x - x_0)/\sigma)$, with x_0 the soliton position and σ its half-width. In Fig. S2(b), we use this single soliton solution to fit the density profile in the nonlinear regime from Fig. 2(b) of the main text. The two soliton dips are fitted independently, using the same soliton width of 5.2 μm. The experimental data is well reproduced by the theoretical profile of two independent solitons in the region between the two excitation beams.

The fits reproduce the presence of the soliton dips on top of a flat background. The dips are separated by 13.5 μm, significantly more than twice their width. This situation is very different to what is observed in the linear regime, Fig. S2(a), in which a standard cosine-like interference pattern is observed with minima separated by exactly twice the FWHM.

These observations evidence that the density dips in the nonlinear regime are indeed solitons. Note that the nonlinear nature of the fluid is also confirmed by the behavior of the measured phase scans, characterized by sharp changes of the profile incompatible with the linear regime (compare Fig. 1(e) and Fig. 3(e) of the main text).

III - POWER-CONTROLLED BISTABILITY OF THE SOLITON TRAIN

A resonantly pumped dissipative nonlinear system, such as a quantum well embedded in a microcavity, in the strong coupling regime, can exhibit bistability when scanning the pumping power upward or downward [2]. In this section, we present experiments revealing that such a bistable behavior is also present in our system. The bistability affects not only the transmitted intensity, but also the field profile in the cavity. We also report a bistability of the soliton pattern, controlled by the pumping power.

Fig. S3(a) presents the evolution of the real space emission profile along the wire, integrated over the transverse direction, in an upward scan of the pumping power. Fig. S3(b) is the corresponding downward scan, with the same experimental parameters and starting from the maximum pumping power reached in the upward scan. $\Delta\varphi$ is fixed to a value close to zero (but non zero). The threshold power corresponding to the transition from the linear to the nonlinear regime, measured at $P = 23$ mW in the upward scan, is lowered in the downward scan to $P = 9$ mW. As one can see in the inset of Fig. S3(b), this behavior corresponds to a standard hysteresis loop.

Focusing now on the evolution of the profile in the nonlinear regime, we notice, in the upward scan, a second transition $P = 28$ mW from a profile containing two solitons directly above threshold, to a profile with zero solitons for higher pumping powers. The mechanism responsible for such a transition has already been discussed in the main text (Fig. 2(e)). In the downward scan however, a profile that contains a single soliton is clearly visible from $P = 27$ mW down to $P = 21$ mW, before the transition to a pattern with two solitons when the power is further decreased. Thus, a bistable behavior of the soliton pattern in the nonlinear regime is identified. Note that the existence of a regime with a single soliton is due to the fact that $\Delta\varphi$ is not exactly 0, which relaxes the parity condition for the polariton fluid. Profiles with an even number of solitons are nevertheless still more fa-

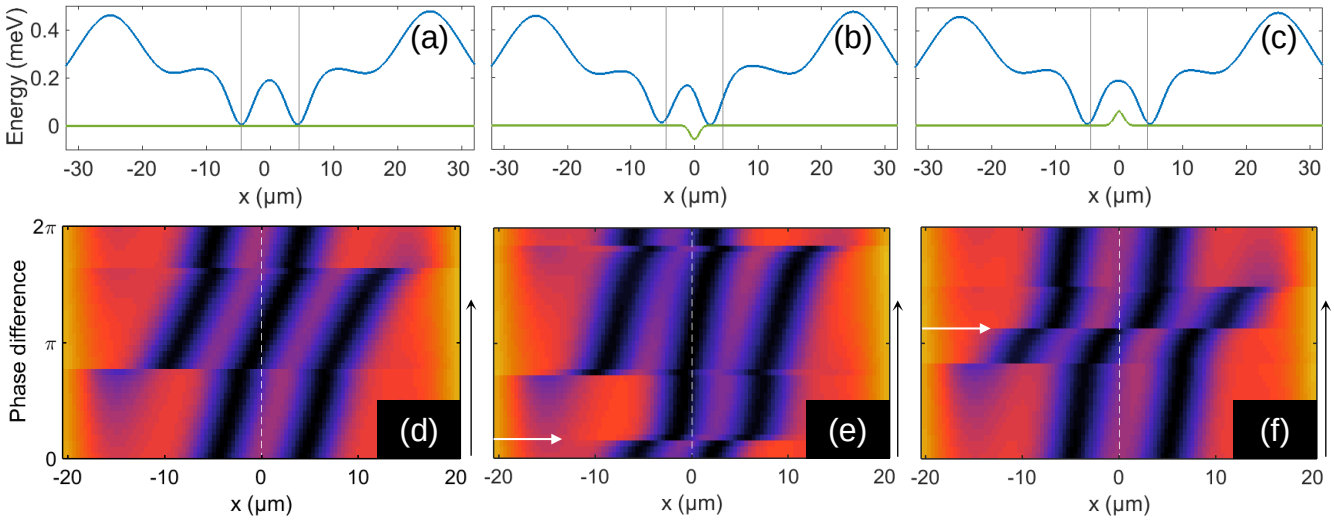

FIG. S4. Top row – Numerical simulations of the density profile in a wire with $\Delta\varphi = 0$ and: (a) no defect. (b) $V_{def} = -60\mu$eV, $x_{def} = 0\mu$m. (c) $V_{def} = 60\mu$eV, $x_{def} = 0\mu$m. On each panel, the blue line is the local interaction energy, proportional to the local polariton density ($E_{int}(x) = \hbar g n(x)$). The green line is the potential energy arising from defects. Gray lines are guides for the eye, indicating the position of the solitons in the profile without defects. Bottom row – Corresponding phase scans in the upward direction. The white dotted line is a guide for the eye, indicating the position of the defect in (e) and (f).

vorable, which is why the profile with a single soliton is not observed in the upward scan.

This power-controlled bistability is the counterpart of the phase-controlled bistability presented in the main text, in the sense that the number of solitons in the wire can be controlled by two independent parameters: the pumping power P, and the phase twist imposed across the wire, $\Delta\varphi$. Tuning either of these parameters, the expulsion or generation of a soliton is an abrupt event inherent to the discrete nature of the solitons, and additionally such a transition is associated with a hysteresis when scanning a single parameter.

IV - INFLUENCE OF DISORDER

In this section, we discuss the influence of disorder in the wire on the soliton train generated in the nonlinear regime. We perform numerical simulations as described in the main text, including an additional potential energy term that accounts for the presence of defects in the wire. A defect is modeled by a gaussian potential:

$$V(x) = V_{def} e^{-\frac{(x-x_{def})^2}{w^2}}, \qquad (1)$$

where the defect depth V_{def} can be either positive or negative, x_{def} is the defect position and w its width.

From the general theory of solitons in atomic Bose gases [3], it is known that for repulsive $V_{def} > 0$ defect potentials, the energy of a dark soliton is minimum when the soliton is located at the defect position where the background atomic density is lower (and viceversa for an attractive defect). This is easily understood in a perturbative picture as the interaction energy with the defect is proportional to the local particle density. On the other hand, the effective mass of a dark soliton seen as a quasiparticle is negative, as intuitively understood from the fact that the dark soliton corresponds to missing particles. As a result, while energy minimization suggests that a dark soliton tends to bind to a repulsive defect, its actual kinematics is characterized by a repulsive acceleration [4].

Even if we are not aware of any complete theoretical study for polariton fluids, we can reasonably expect that these features remain valid also in this case. As the dissipative nature of these systems reduces the importance of energetic arguments, the physics is however likely to be dominated by the kinetic aspects and our simulations appear to confirm this naive expectation.

Fig. S4(a-c) present the results of numerical simulations carried out with various defects (b,c), compared to a simulation without defects (a). The latter corresponds to the simulation of Fig. 2(c) of the main text. In both Fig. S4(b) and (c), the defect width is $w = 1$ μm. It is clearly visible that the presence of defects modifies the position of the solitons in the wire. More precisely, a negative defect has an attractive effect for a soliton, while a positive defect repels solitons.

Fig. S4(d-f) shows numerical simulations of the evolution of the soliton pattern in a scan of $\Delta\varphi$, highlighting the effect of disorder on the soliton train position.

As discussed in the main text, the displacement of the soliton pattern, shifted rightwards as $\Delta\varphi$ is increased, is homogeneous in the scan with no defects (d).

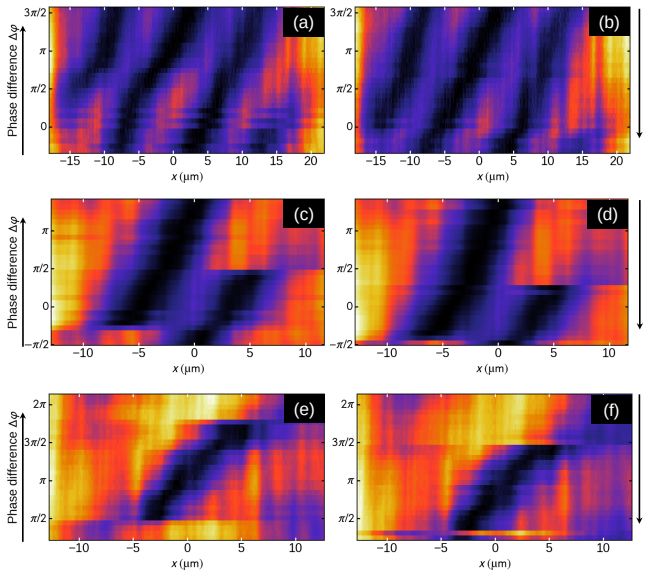

FIG. S5. Left column – Phase scans in the upward direction ($\Delta\varphi$ increasing). Right column – Corresponding phase scans in the downward direction. The parameters for each scans are: (a),(b) $\Delta E = 0.21$ meV, $P = 42$ mW, $d = 60$ μm. (c),(d) $\Delta E = 0.35$ meV, $P = 90$ mW, $d = 40$ μm. (e),(f) $\Delta E = 0.20$ meV, $P = 103$ mW, $d = 40$ μm. Panels (a), (b) (resp. (c),(d) and (e),(f)) correspond to Fig. 4(b) (resp. (c) and (d)).

In the case of a negative defect (e), the displacement is distorted: due to the attractive effect of the negative defect, a soliton coming close to the defect position is pinned and stays at the defect position in a finite range of $\Delta\varphi$. Beyond a threshold value of $\Delta\varphi$, the soliton is abruptly depinned as indicated by a white arrow in Fig. S4(e). Such behavior is very close to the one experimentally observed and shown in Fig.3.(e),(f) of the main text.

For a positive defect on the other hand (f), there is no value of $\Delta\varphi$ for which a soliton is at the defect position, confirming the repulsive effect of the potential step. Moreover, because of this repulsion, an abrupt jump of the soliton pattern is observed, with a soliton jumping from the left of the defect to its right (indicated by the white arrow), when $\Delta\varphi$ is increased to the point that the solution with two solitons on the right of the defect becomes more stable than two solitons on the left.

This interpretation in terms of disorder is further supported by the observation that different sections of the sample showed slightly different soliton profiles while keeping the same excitation conditions.

Note that the values of $\Delta\varphi$ corresponding to the generation and expulsion of a soliton are affected by the presence of a defect. In particular, the hysteresis range measured during a phase scan depends significantly on the disorder in the wire.

IV - PHASE SCANS FOR VARIOUS SOLITON TRAINS

The number of solitons in the wire can be controlled by tuning the experimental parameters. Fig. S5 presents the phase scans, at constant pumping power, in the upward and downward direction, that correspond to the plots of Fig. 4 (b–d) of the main text. Parameters are indicated in the caption.

[1] L. Pitaevskii and S. Strindgari, *Bose-Einstein Condensation*, 1st ed. (Clarendon Press, Oxford, 2003).

[2] A. Baas, J. P. Karr, H. Eleuch, and E. Giacobino, Phys. Rev. A **69**, 23809 (2004).

[3] V. V. Konotop and L. Pitaevskii, Phys. Rev. Lett. **93**, 240403 (2004).

[4] D. J. Frantzeskakis, G. Theocharis, F. K. Diakonos, P. Schmelcher, and Y. S. Kivshar, Phys. Rev. A **66**, 053608 (2002).